

A.S. Vakula¹, O.A. Kravchuk², S.I. Tarapov^{1,2,3}, A.G. Belous⁴

¹ O.Ya. Usikov Institute of Radiophysics and Electronics
12, Acad. Proskury St., Kharkiv, 61085, Ukraine
E-mail: vakula@ire.kharkov.ua

² Kharkiv National University of Radio Electronics
14, Nauky Ave., Kharkiv, 61166, Ukraine

³ V.N. Karazin Kharkiv National University
4, Svobody Sq., Kharkiv, 61022, Ukraine

⁴ Institute of General and Inorganic Chemistry,
32/34, Akad. Palladina Ave., Kyiv, 03142, Ukraine

Ferromagnetic resonance in $\text{Fe}_{1-x}\text{Co}_x\text{Fe}_2\text{O}_4$ nanoparticles precipitated from diethylene glycol

Subject and Purpose. One of the ways to gain in the efficiency of the hyperthermia technique is through the synthesis of new magnetic nanomaterials offering high coercive force without affecting biocompatibility. A proven technology is the doping of biocompatible materials, such as Fe_3O_4 , with atoms of highly coercive substances, such as Co atoms. Despite it has been the theme of much investigation, magnetic state of such nanoparticles is still not completely understood. The present study is devoted to the magnetic and magnetic resonance properties of $\text{Fe}_{1-x}\text{Co}_x\text{Fe}_2\text{O}_4$ nanoparticles synthesized by the precipitation from diethylene glycol at two, $T = 200^\circ\text{C}$ and 500°C , temperatures. The purpose is to study magnetic and magnetic resonance properties of $\text{Fe}_{1-x}\text{Co}_x\text{Fe}_2\text{O}_4$ nanoparticles at various concentrations x .

Method and Methodology. The magnetometric method and the electron spin resonance method were employed to obtain, correspondingly, magnetic hysteresis loops of magnetic nanoparticles and ferromagnetic resonance (FMR) spectra in the frequency band $f = 8 \dots 20$ GHz at the temperature $T = 294$ K. Transmission electron microscopy was used for nanoparticle observations.

Results. The analysis of the measuring results has shown that among $\text{Fe}_{1-x}\text{Co}_x\text{Fe}_2\text{O}_4$ nanoparticle samples with concentrations $x = 0.0, 0.5, \text{ and } 1.0$, the total magnetic anisotropy field at $x = 0.5$ is the largest of the three because its crystalline anisotropy field is the largest compared to $x = 0.0$ and 1.0 .

Conclusion. The presented results have advanced our understanding of the fundamental interaction between magnetic Co and Fe atoms inside the crystal lattice of AFe_2O_4 , where A is Co or Fe. The gained knowledge can contribute to the development of magnetically controlled high-frequency filters and frequency selectors. Fig. 5. Table 1. Ref.: 19 items.

Key words: electron spin resonance, ferromagnetic resonance, magnetite, microwaves.

The interest in magnetic nanoparticles (MNP) is on the rise [1] due to their versatile applications including, first of all, telecommunications (fiber-optic communication lines, antenna-feeder devices, etc.) and medicine where active use of nanoparticles is expected in cancer treatment. In it, magnetic nanoparticles can be both chemotherapeutic drug carriers in the targeted drug delivery methods [2–4] and agents in the hyperthermia technique [5, 6]. In the latter, nanoparticles are heated by an external high-frequency magnetic field in order to

destroy malignant tumor cells under the influence of heat. Unfortunately, many sorts of nanoparticles created from biocompatible (nontoxic) materials turn out to be ineffective in hyperthermia because their coercive force is low. So, neither the constant magnetic field control nor the nanoparticle heating with an alternating magnetic field can work properly. To our knowledge, this problem has not been solved to date. An apparent approach to the problem solution is to incorporate foreign, highly coercive atoms into a biocompatible MNP. Thus,

highly coercive cobalt (Co) atoms can be doped into biocompatible, say Fe_3O_4 , nanoparticles [7, 8]. This approach does not affect the biocompatibility but improves the heating efficiency of the magnetic nanoparticles. The necessary values, such as coercive force, H_C , total magnetic anisotropy field, H_a , and magnetization, M , can be obtained from the ferromagnetic resonance (FMR) spectrum and from the shape of the magnetic hysteresis loop [9–11].

Magnetic $Fe_{1-x}Co_xFe_2O_4$ nanoparticles synthesized by the precipitation from diethylene glycol will be examined for their magnetic properties in an effort to find how the Fe–Co atom substitution acts on the FMR spectrum and shape of the magnetic hysteresis loop. To this end, the measurements of FMR spectra and magnetic hysteresis loops were performed for $Fe_{1-x}Co_xFe_2O_4$ nanoparticles with the three Co concentrations $x = 0.0$, 0.5, and 1.0.

1. Theory. For the studied MNP samples, the FMR frequency is related to the external magnetic field as [12]

$$f_{res} = \frac{\gamma}{2\pi}(H - H_a),$$

where f_{res} is the FMR frequency, γ is the gyromagnetic ratio, H is the external static (or slowly varying in magnitude) magnetic field applied to the sample, and H_a is the total magnetic anisotropy field. The H_a field can be represented as a sum of the field H_{dip} of the dipole-dipole interaction between magnetic nanoparticles, the magnetocrystalline anisotropy field (H_K), and the surface anisotropy field (H_S) [13]. An assumption is made that the nanoparticles and clusters of the nanoparticles are spherically shaped (or almost spherically), which makes the shape anisotropy of the H_a field negligible with demagnetizing factors approximately equal in all the Cartesian directions. We also assume that the contributions to H_a from the other anisotropy fields are insignificant [13]. In particular, each contribution to H_a is a function of M which, in turn, depends on the concentration x . The H_K field involves the magnetocrystalline anisotropy constant, K , [13] which is associated with x , too. Based on the experimental results, a contribution from each of the anisotropy fields will be estimated in the case of mutually interacting $Fe_{1-x}Co_xFe_2O_4$ nanoparticles.

2. Results and discussions. The samples of $Fe_{1-x}Co_xFe_2O_4$ nanoparticles were synthesized by the precipitation from the diethylene glycol solution at the two temperatures $T = 200$ °C and $T = 500$ °C (see the Table). The initial reagents were metal nitrates $Fe(NO_3)_3 \cdot 9H_2O$ and $Co(NO_3)_2 \cdot 6H_2O$ (analytical stage). The precipitant was NaOH (97% purity), the precipitation process was held in the argon environment. An extended description of the synthesis process can be found in [12, 13].

The MNP morphology and size (Fig. 1) were studied using a transmission electron microscope JEM-1230. The TEM images (Fig. 1, *a–c*) were analyzed for the MNP size distribution by the procedure described in [7]. The MNP magnetic research was performed using a commercial Quantum Design Magnetic Property Measurement System adapted to the temperature range $T = 2 \dots 300$ K.

The FMR properties of $Fe_{1-x}Co_xFe_2O_4$ nanoparticles were studied in the frequency band $f = 8 \dots 40$ GHz at the temperature $T = 300$ K. Each MNP sample enclosed in a spherical dielectric container was placed inside a tunable rectangular microwave cavity resonator [7, 14] inserted between the poles of the electromagnet and connected to the spectrometer [10, 15]. The MNP samples were examined in scanning mode by applying an external magnetic field in the range $H = 0 \dots 10$ kOe. The experimentally obtained FMR spectra for #1 and #3 (two MNP synthesis temperatures) are shown in Fig. 2.

Fig. 3 shows the hysteresis loops of the studied nanoparticles. From Figs. 2 and 3, the contribution from each magnetic anisotropy field can be estimated.

We found that a 5-fold increase of the MNP size raises H_a 2.7 times. In so far as the M value also increases 2.7 times, it can be concluded that it is the field H_{dip} of the dipole-dipole interaction that mainly contributes to H_a at $T = 300$ K since H_a

Parameters of the Samples

Samples	#1 Fe_3O_4	#2 $CoFe_2O_4$	#3 Fe_3O_4	#4 $Fe_{0.5}Co_{0.5}Fe_2O_4$
MNP average size d , nm	4	4	20	20
Synthesis temperature T , °C	200	200	500	500
Co concentration	0.0	1.0	0.0	0.5

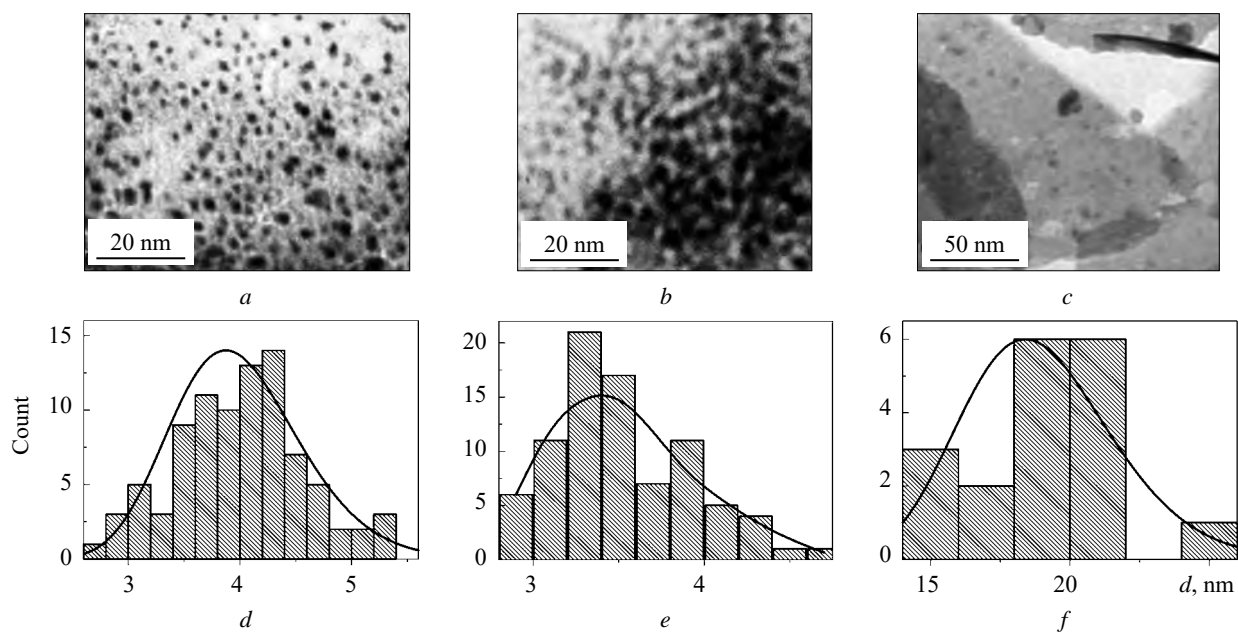


Fig. 1. Photographs of MNP samples: *a* – sample #1, *b* – sample #2, and *c* – sample #4 and diagrams (*d*, *e*, *f*) of MNP size distribution for $x = 0.0$, $x = 1.0$ and $x = 0.5$

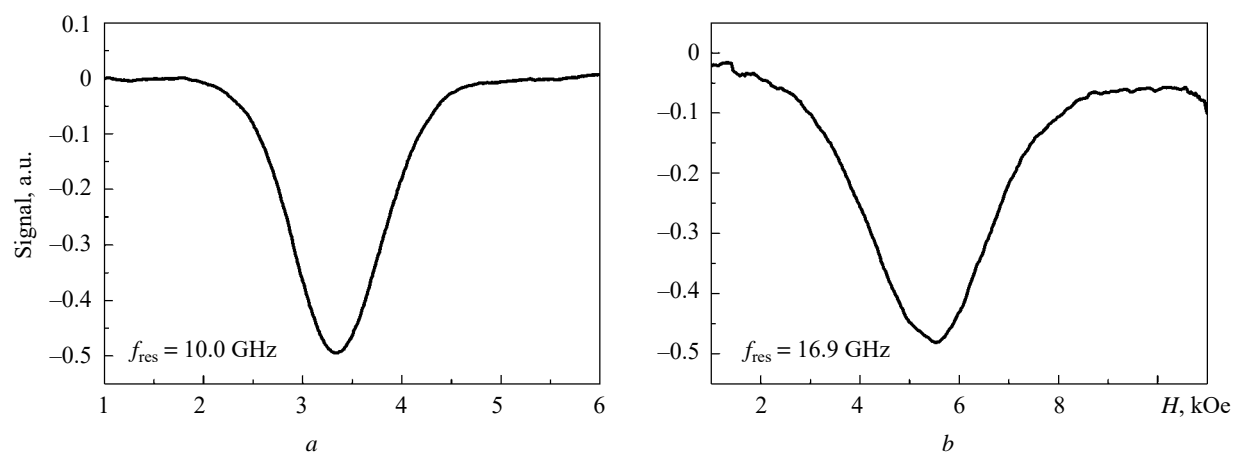


Fig. 2. FMR spectra from Fe_3O_4 nanoparticles ($x = 0.0$) synthesized at the temperatures: $T = 200$ °C, sample #1 (*a*) and $T = 500$ °C, sample #3 (*b*)

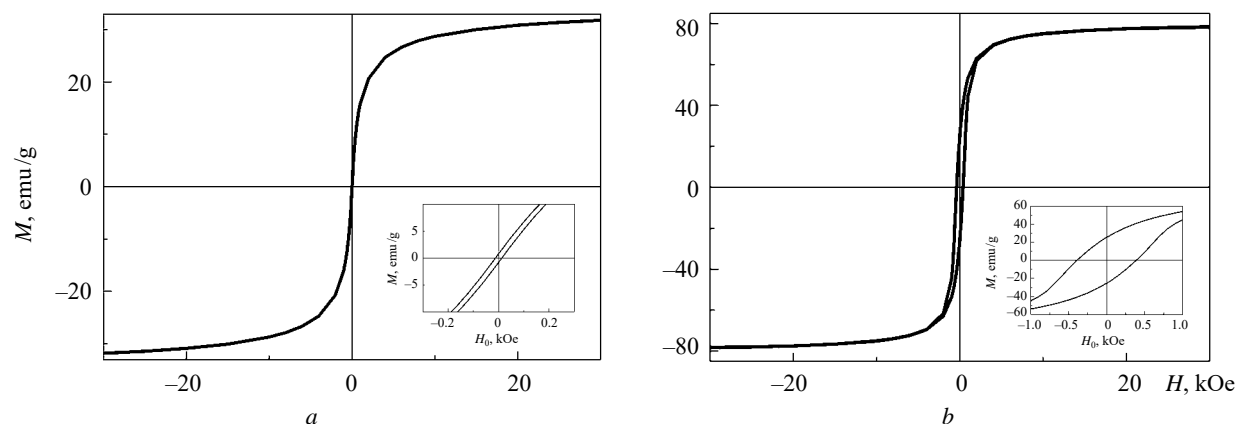


Fig. 3. Magnetic hysteresis loops of Fe_3O_4 nanoparticles ($x = 0.0$) synthesized at the temperatures: $T = 200$ °C, sample #1 (*a*) and $T = 500$ °C, sample #3 (*b*)

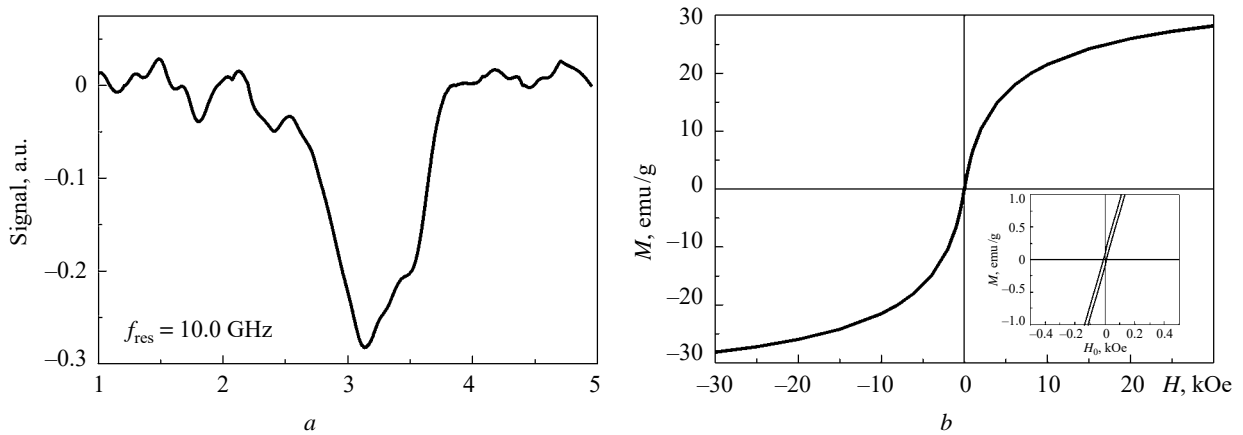


Fig. 4. FMR spectrum (a) and magnetic hysteresis loop (b) of $CoFe_2O_4$ nanoparticles ($x = 1.0$) synthesized at $T = 200$ °C, sample #2

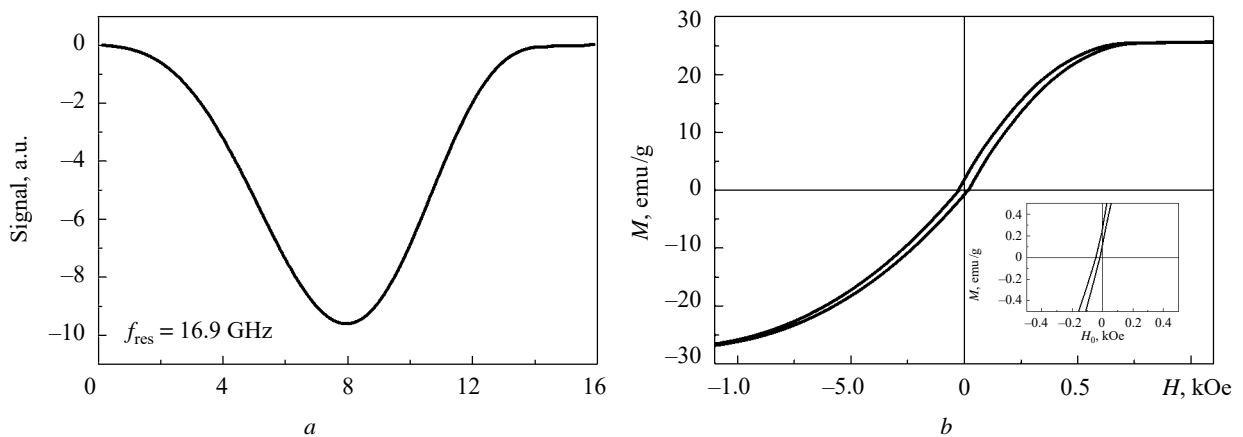


Fig. 5. FMR spectrum (a) and magnetic hysteresis loop (b) of $Fe_{0.5}Co_{0.5}Fe_2O_4$ nanoparticles synthesized at $T = 500$ °C, sample #4

directly depends on M . The H_K field remains unchanged as the MNP crystal structure is immune to the MNP size [13]. For the MNP size values indicated in the Table, the H_S field also contributes scarcely anything to H_a .

Fig. 4 shows the FMR spectrum and the magnetic hysteresis loop of $CoFe_2O_4$ nanoparticles synthesized at $T = 200$ °C (sample #2).

A comparison of the experimental results for samples #1 (Figs. 2, a and 3, a) and #2 (Fig. 4) suggests that the Fe–Co atom substitution raises the H_a field not only due to the M increase (Fig. 4, b) but also owing to the increase of the H_K field [13].

The FMR spectral line is explained by a significant MNP size dispersion, which is also confirmed by the TEM images (Fig. 1, a–c).

A similar comparison of the experimental results for samples #3 (Fe_3O_4) and #4 ($Fe_{0.5}Co_{0.5}Fe_2O_4$)

synthesized at $T = 500$ °C reveals that M for #3 increases (Fig. 5).

We found that the FMR linewidth of #4 ($Fe_{0.5}Co_{0.5}Fe_2O_4$) is two times the FMR linewidth of #3 (Fe_3O_4). The broadening of the FMR spectral line indicates poor collinearity of the MNP spin system and a significant MNP size dispersion.

The H_a field value of $Fe_{0.5}Co_{0.5}Fe_2O_4$ nanoparticles is 25% higher than that of $CoFe_2O_4$ [16]. We suppose that the contribution from both Fe^{2+} and Co^{2+} ions affect the magnetocrystalline anisotropy constant K which is involved in H_K and, consequently, H_a [17, 18] and plays an important role.

3. Conclusions. The magnetic resonance study of the Fe–Co atom substitution in $Fe_{1-x}Co_xFe_2O_4$ nanoparticles has brought the following results.

The total magnetic anisotropy field H_a increases by 2.7 times as the MNP average diameter increases from 4 to 20 nm. It is mainly due to that the

magnetization M and the field H_{dip} of dipole-dipole interaction between nanoparticles increase.

The Fe–Co atom substitution raises the magnetization M by up to 60% as the concentration x in $\text{Fe}_{0.5}\text{Co}_{0.5}\text{Fe}_2\text{O}_4$ nanoparticles changes from $x = 0.0$ to $x = 1.0$. This is accompanied by a three-fold increase of the H_a field and can most probably be caused by the increase of the magnetocrystalline anisotropy field H_K .

As the concentration changes from $x = 0.0$ to $x = 0.5$ the magnetization M is lowered by a factor of 2.5, and H_a reduces to one-fourth of its previous value. This suggests that the contributions from both Fe^{2+} and Co^{2+} ions affect the magnetocrystalline anisotropy field H_K .

Acknowledgement. *The authors are grateful to Prof. N.N. Beletskii for his valuable comments and helpful assistance during this work.*

REFERENCES

1. Mozul, K.A., Olkhovik, L.P., Sizova, Z.I., 2013. Surface magnetic anisotropy of CoFe_2O_4 nanoparticles with giant low-temperature hysteresis. *Low Temperature Phys.*, **39**(4), pp. 469–474 (in Russian).
2. Hafeli, U., Schott, W., Teller, J., 1997. *Scientific and clinical applications of magnetic carriers*. New York: Springer. 610 p.
3. Torres, T.E., Roca, A.G., Morales, M.P., Ibarra, A., Marquina, C., Ibarra, M.R. and Goya, G.F., 2010. Magnetic properties and energy absorption of CoFe_2O_4 nanoparticles for magnetic hyperthermia. *J. Phys.: Conf. Ser.*, **200**, pp. 072101 (4 p.). DOI: 10.1088/1742-6596/200/7/072101.
4. Tartaj, P., Morales, M.P., Veintemillas-Verdaguer, S., Gonzalez-Carreño, T., Serna, C.J., 2006. Synthesis, properties and biomedical applications of magnetic nanoparticles. In: *Handbook of magnetic materials*, **16**, pp. 403–482. Ch. 5. DOI: 10.1016/S1567-2719(05)16005-3.
5. Gandha, K., Elkins, K., Poudyal, N., Liu, J.P., 2015. Synthesis and characterization of CoFe_2O_4 nanoparticles with high coercivity. *J. Appl. Phys.*, **117**(17), 17A736. DOI: <https://doi.org/10.1063/1.4916544>.
6. Bañobre-López, M., Teijeiro, A., Rivas, J., 2013. Magnetic nanoparticle-based hyperthermia for cancer treatment. *Rep. Pract. Oncol. Radiother.*, **18**(6), pp. 397–400. DOI: <https://doi.org/10.1016/j.rpor.2013.09.011>.
7. Vakula, A.S., 2015. Temperature dependent microwave properties of Fe_3O_4 nanoparticles synthesized by various techniques. *Radiophys. electron.*, **6**(20)(3), pp. 62–65 (in Russian). DOI: <https://doi.org/10.15407/rej2015.03.062>.
8. Singh, A.K., Srivastava, O.N., Singh, K., 2017. Shape and Size-Dependent Magnetic Properties of Fe_3O_4 Nanoparticles Synthesized Using Piperidine. *Nanoscale Res. Lett.*, **12**(1), pp. 298–305. DOI: 10.1186/s11671-017-2039-3.
9. Poole, C., 1997. *Electron Spin Resonance: A comprehensive treatise on experimental techniques*. New York: Dover Publ.
10. Vakula, A., Bereznyak, E., Gladkovskaya, N., Dukhopelnikov, E., Herus, A., Tarapov, S., 2016. Spectral investigation of magnetite nanoparticles interaction with charged drugs. In: *9th Int. Kharkiv Symposium on Physics and Engineering of Microwaves, Millimeter and Submillimeter Waves (MSMW 2016)*. Proc. Kharkiv, Ukraine, 21–24 June 2016. Kharkiv: IEEE. A-30.
11. Shabarchina, M.M., Tsapina, A.I., Malenkov, A.G., Vanin, A.F., 1990. The behavior of magnetic metallic iron particles in animals. *Biofizika*, **35**(6), pp. 985–988 (in Russian).
12. Yelenich, O.V., Solopan, S.O., Trachevskii, V.V. and Belous, A.G., 2013. Synthesis and Properties of AFe_2O_4 ($\text{A} = \text{Mn}, \text{Fe}, \text{Co}, \text{Ni}, \text{Zn}$) Nanoparticles Produced by Deposition from Diethylene Glycol Solution. *Russ. J. Inorg. Chem.*, **58**(8), pp. 901–905. DOI: <https://doi.org/10.1134/S0036023613080068>.
13. Gubin, S.P., Koksharov, Yu.A., Khomutov, G.B., Yurkov, G.Yu., 2005. Magnetic nanoparticles: production methods, structure and properties. *Russ. Chem. Rev.*, **74**(6), pp. 539–574. DOI: 10.1070/RC2005v074n06ABEH000897.
14. Tarapov, S.I., Machekhin, Yu.P., Zamkovoy, A.S., 2008. *Magnetic Resonance for Optoelectronic Materials Investigating*. Kharkov: Collegium. 144 p. ISBN 978-966-8604-42-3.
15. Chi-Kuen Lo, 2013. *Instrumentation for Ferromagnetic Resonance Spectrometer*. In: Orhan Yalcin, ed. 2013. *Ferromagnetic Resonance - Theory and Applications*. Publisher: InTech. Ch. 2, pp. 47–62. DOI: <http://dx.doi.org/10.5772/56069>.
16. Morgunov, R.B., Dmitriev, A.I., Dzhardimalieva, G.I., Pomogaïlo, A.D., Rozenberg, A.S., Tanimoto, Y., Leonowicz, M., Sowka, E., Ferromagnetic resonance of cobalt nanoparticles in a polymer shell. *Phys. Solid State*, **49**(8), pp. 1436–1441 (in Russian).
17. Krupichka, S., 1976. *Physics of ferrites and related magnetic oxides*. Translated from German. Moscow: Mir Publ. Vol. 2 (in Russian).
18. Durneata, D., Hempelmann, R., Caltun, O. and Dumitru, I., 2014. High-Frequency Specific Absorption Rate of $\text{Co}_x\text{Fe}_{1-x}\text{Fe}_2\text{O}_4$ Ferrite Nanoparticles for Hyperthermia Applications. *IEEE Trans. Magn.*, **50**(11), pp. 5201104 (4 p.). DOI: 10.1109/TMAG.2014.2324011.

Received 15.04.2020

А.С. Вакула¹, О.О. Кравчук², С.І. Таранов^{1,2,3}, А.Г. Білоус⁴

¹ Інститут радіофізики та електроніки ім. О.Я. Усикова НАН України
12, вул. Акад. Проскури, Харків, 61085, Україна

² Харківський національний університет радіоелектроніки
14, просп. Науки, Харків, 61166, Україна

³ Харківський національний університет імені В.Н. Каразіна
4, майдан Свободи, Харків, 61022, Україна

⁴ Інститут загальної та неорганічної хімії
32/34, просп. Акад. Палладіна, Київ, 03142, Україна

ФЕРОМАГНІТНИЙ РЕЗОНАНС У НАНОЧАСТИНКАХ
 $Fe_{1-x}Co_xFe_2O_4$, ОСАДЖЕНИХ З ДІЕТИЛЕНГЛІКОЛЮ

Предмет і мета роботи. Одним із шляхів підвищення ефективності методики гіпертермії є спосіб синтезу нових магнітних наноматеріалів. Такі наноматеріали повинні мати високу коерцитивну силу водночас зі збереженням біосумісності. Надійним способом є допування біосумісних матеріалів, таких як Fe_3O_4 , атомами речовин з великою коерцитивною силою – наприклад, атомами Со. Відомі на цей час роботи інших авторів недостатньо повно відображають магнітний стан подібних наночастинок. Таким чином, предметом нашого дослідження є магнітні та магніторезонансні властивості наночастинок $Fe_{1-x}Co_xFe_2O_4$, синтезованих шляхом осадження з діетиленгліколю за температури $T = 200$ К та $T = 500$ К. Метою роботи є визначення залежності магнітних та магніторезонансних властивостей $Fe_{1-x}Co_xFe_2O_4$ зі зміною x .

Метод і методологія роботи. Методом електронного спінового резонансу в діапазоні $8 \dots 20$ ГГц при $T = 294$ К зареєстровано спектри феромагнітного резонансу. Магнітометричним методом досліджено петлі магнітного гістерезису наночастинок; методом просвічувальної електронної мікроскопії отримано фотографії магнітних наночастинок.

Результати роботи. Аналіз результатів експериментальних досліджень зразків наночастинок $Fe_{1-x}Co_xFe_2O_4$ ($x = 0,0; 0,5; 1,0$) показав, що підвищене значення сумарного поля магнітної анізотропії в наночастинках $Fe_{1-x}Co_xFe_2O_4$ з концентрацією $x = 0,5$ у порівнянні з $x = 0,0$ та $x = 1,0$ викликане збільшенням поля кристалографічної анізотропії.

Висновок. Результати представлених досліджень дозволять визначити фундаментальну взаємодію магнітних атомів Со та Fe у кристалічній ґратці. Отримані знання будуть корисними у розробленні магнітокерованих високочастотних фільтрів та частотних селекторів.

Ключові слова: електронний спіновий резонанс, феромагнітний резонанс, магнетит, надвисокі частоти.